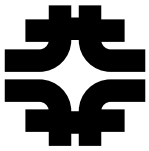

Fermi National Accelerator Laboratory

FERMILAB-Conf-96/171-E
CDF

Recent Top Quark Physics Results at the Tevatron

Juan A. Valls
For the CDF Collaboration

Fermi National Accelerator Laboratory
P.O. Box 500, Batavia, Illinois 60510

July 1996

Invited Talk at the *XXIV International Meeting on Fundamental Physics, From the Tevatron to the LHC*, Playa de Gandia, Spain, April, 1996

Operated by Universities Research Association Inc. under Contract No. DE-AC02-76CHO3000 with the United States Department of Energy

Disclaimer

CDF/DOC/TOP/PUBLIC/3737
June 28, 1996

Recent Top Quark Physics Results at Tevatron

Juan A. Valls [1]
Fermilab

Invited talk at the XXIV International Meeting on Fundamental Physics,
"From the Tevatron to the LHC"
April 1996, Playa de Gandía, Spain.

Abstract

The evidence of top quark pair production in $p\bar{p}$ collisions has been firmly established by both the CDF and the DØ collaborations at Fermilab. In this paper the latest top quark physics results from both experiments at the Tevatron Collider are presented. The experimental analyses have concentrated in improving the accuracy of top quark production and decay measurements like cross sections, mass and branching fractions. The results shown correspond to the final data set collected with both detectors during the complete Tevatron Run I. This represents a total recorded integrated luminosity of $\sim 110\ pb^{-1}$ for CDF and $\sim 100\ pb^{-1}$ for DØ .

[1]Visitor from IFIC, Centro mixto CSIC-Universidad de Valencia, Dr. Moliner 50, E-46100, Burjassot, Valencia, Spain.

1 Introduction

In April 1994 CDF [1] published the first experimental evidence of the existence of the top quark. Later, in 1995, this evidence became a discovery when both the CDF and DØ collaborations confirmed its presence by analyzing a larger data sample [2, 3]. One year since the top quark discovery announcement, the focus on top quark physics has changed from demonstrating the evidence of its presence to addressing, with the best possible accuracy, all top quark production and decay properties like cross sections, mass and branching fractions.

In this paper a summary of the more recent results on top quark physics from both experiments is presented. Main emphasis is given to the CDF results followed by a few highlights of the DØ analysis used for comparison. The paper is organized as follows: in Section 2 top quark production and decay characteristics at Tevatron are summarized. The Tevatron and the CDF and DØ detectors are briefly described in Section 3 and 4. The counting experiments and the cross section analysis are covered in Section 5. The mass measurement is presented in Section 6. Section 7 and 8 are devoted to the description of the work done on top kinematics and decay studies so far and finally, the conclusions and future prospects are outlined in Section 9.

2 Top Quark Production and Decays

At Tevatron top quarks are produced mainly in pairs through gluon-gluon fusion and $q\bar{q}$ annihilation, the latter being the dominant production mechanism with a 90% probability. Single top quarks may also be produced through W gluon fusion or s-channel W production although the cross sections for these processes are estimated to be one or two orders of magnitude below the $t\bar{t}$ production respectively at Tevatron energies [4].

As a consequence of the high mass of the top quark, its expected lifetime becomes shorter than the time needed for hadronization, so it decays before fragmentation takes place. Within the framework of the Standard Model, top quarks decay almost exclusively into a W boson and a b quark. The W bosons subsequently decay either to a lepton and a neutrino or to a quark and antiquark. This is shown in Figure 1 for the particular case in which both W's decay leptonically. Final state quarks from the W decays, as well as b quarks from the top decays, hadronize to jets. Depending on the decay mode of the W, top quark pair decays can be categorized as:

1) Dilepton channel: both W^+ and W^- decay to an electron or a muon. This mode has a branching fraction of about 5% leading to rather clean topologies with two high transverse momentum leptons, missing transverse energy ($\not\!\!E_T$) carried off by neutrinos and at least 2 jets in the final state.

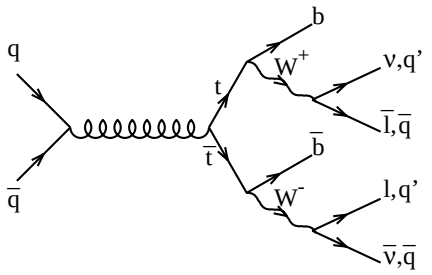

Figure 1: *Tree level top quark pair production through $q\bar{q}$ annihilation followed by the Standard Model top quark decay chain.*

Decay Mode	Process	Branching Ratio
All Hadronic Channel $\sim 44\%$	$t\bar{t} \to (q\bar{q}'b)(q\bar{q}'\bar{b})$	$36/81 = 44.4\%$
Lepton (e+μ) + jets Channel $\sim 30\%$	$t\bar{t} \to (q\bar{q}'b)(e\nu\bar{b})$ $t\bar{t} \to (q\bar{q}'b)(\mu\nu\bar{b})$	$12/81 = 14.8\%$ $12/81 = 14.8\%$
Tau + jets Channel $\sim 15\%$	$t\bar{t} \to (q\bar{q}'b)(\tau\nu\bar{b})$	$12/81 = 14.8\%$
Dilepton Channel $\sim 5\%$	$t\bar{t} \to (e\nu b)(\mu\nu\bar{b})$ $t\bar{t} \to (e\nu b)(e\nu\bar{b})$ $t\bar{t} \to (\mu\nu b)(\mu\nu\bar{b})$	$2/81 = 2.5\%$ $1/81 = 1.2\%$ $1/81 = 1.2\%$
Tau Lepton (e+μ) Channel $\sim 5\%$	$t\bar{t} \to (e\nu b)(\tau\nu\bar{b})$ $t\bar{t} \to (\mu\nu b)(\tau\nu\bar{b})$	$2/81 = 2.5\%$ $2/81 = 2.5\%$
Tau-Tau Channel $\sim 1\%$	$t\bar{t} \to (\tau\nu b)(\tau\nu\bar{b})$	$1/81 = 1.2\%$

Table 1: *Decay modes for a $t\bar{t}$ pair and their lowest order branching ratios assuming Standard Model decays. q stands for light quarks: u, d, c and s.*

2) Lepton + jets channel: here only one of the W bosons decay leptonically to an e or μ while the other decay hadronically. The final state includes a high p_T charged lepton, an imbalance from the undetected neutrino ($\not\!\!E_T$) and four or more jets from the hadronization of the quarks. The branching fraction is $\sim 30\%$.

3) Hadronic channel: in this mode both W bosons decay to a quark and an antiquark pair. This happens with the largest probability, about 44% of the time, but a formidable background from other QCD multijet processes overwhelms the signal.

The approximate branching fractions for the different decay modes are listed in Table 1. Other channels also being investigated include the observation of τ hadronic decays of the W boson (tau lepton channel).

3 The Tevatron Collider

The Tevatron Collider is a 6.3 Km circumference $p\bar{p}$ storage ring that generates collisions at a center of mass energy of 1.8 TeV . The Tevatron operates with 6 bunches of protons and 6 bunches of counter-rotating antiprotons crossing each 3.5 μsec at two interaction points where the CDF and DØ detectors are located. Right above the Tevatron ring sits the Main Ring, a proton-synchrotron that preaccelerates the beams to 150 GeV.

During the last running period, Run IB (see table below), highest instantaneous Tevatron luminosities reached $2.5 \times 10^{31} cm^{-2} sec^{-1}$. At this luminosity there were, on average, two interactions per crossing. The Tevatron Run I started delivering data in December 1992 and finished in February 1996. During this long run a total of $\sim 110\ pb^{-1}$ and $\sim 100\ pb^{-1}$ of data were accumulated by the CDF and DØ experiments respectively in two running periods:

Run	Start	End	Collected CDF $\int \mathcal{L}$	Collected DØ $\int \mathcal{L}$
Run IA	December 1992	August 1993	$\sim 19.3\, pb^{-1}$	$\sim 15\, pb^{-1}$
Run IB	August 1994	February 1996	$\sim 90\, pb^{-1}$	$\sim 85\, pb^{-1}$

4 The CDF and DØ Experiments

4.1 The CDF Detector

CDF [5] is a general purpose detector designed to efficiently identify leptons and hadronic jets produced in $p\bar{p}$ interactions. It consists of a high precision tracking system contained in a 1.4 T solenoidal magnetic field. Surrounding the solenoid are hermetic sample calorimeters to measure electromagnetic and hadronic energy of electrons and jets, respectively. A perspective view of the detector is shown in Figure 2.

The tracking system consists of three independent devices arranged coaxial to the interaction point. Surrounding the 1.9 cm radius beryllium beampipe is a four layer silicon microstrip vertex detector (SVX) that was installed in 1992. The SVX single hit position resolution is measured to be $\sigma = 13\,\mu$m and the impact parameter resolution at high momenta is measured to be $\sigma = 17\,\mu$m.

Figure 2: *A perspective view of the CDF detector. Shown are the central detectors and the forward and backward detectors.*

A set of Vertex Time Projection Chambers (VTX) reconstruct intermediate tracks in the $r-z$ plane. Surrounding both the SVX and VTX is the Central Tracking Chamber (CTC), a 3.2 m long cylindrical drift chamber with 84 layers of sense wires. It has an outer radius of 1.32 m corresponding to a pseudorapidity coverage of $|\eta| < 1.0$. The resulting momentum resolution in the transverse plane when combining information from all subsystems is $\delta p_T/p_T^2 \sim 0.001\,\mathrm{GeV}^{-1}c$.

Central calorimetry in the region $|\eta| < 1.1$ is provided by a central electromagnetic and hadron calorimeter with projective towers segmented in $\Delta\eta \times \Delta\phi = 0.11 \times 15^\circ$. The sampling medium is composed of scintillators layered with lead and steel absorbers. Plug and Forward calorimeters instrument the region $1.1 < |\eta| < 4.2$ and consist of gas proportional chambers as active media and lead and iron as absorber material. Showers are detected with proportional wire chambers. The overall resolution of the CDF central calorimeters is:

$$\frac{\sigma_E}{E} = \frac{13.5\%}{\sqrt{E_T}} \oplus 2\% \qquad \text{for electromagnetic showers}$$

$$\frac{\sigma_E}{E} = \frac{75\%}{\sqrt{E_T}} \oplus 3\% \qquad \text{for hadrons}$$

Located outside the calorimeter volume are planar drift muon chambers for muon identification allowing precise muon momentum both in the central ($|\eta| < 0.6$), extended ($0.6 < |\eta| < 1.1$) and forward regions.

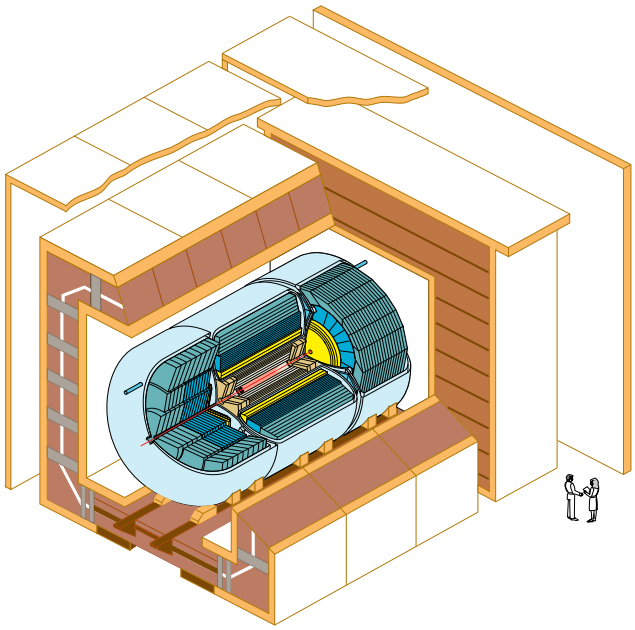

Figure 3: *Cutaway isometric view of the DØ detector.*

4.2 The DØ Detector

The DØ detector [6] was designed with a uniform, hermetic, highly segmented calorimeter as the core of the system ($\Delta\eta \times \Delta\phi = 0.1 \times 6°$ and $|\eta| < 4$). The calorimeter employs up to nine interaction lengths of Uranium absorber and a liquid Argon readout system. A general view of the detector is shown in Figure 3.

The overall resolution of the DØ calorimeter is:

$$\frac{\sigma_E}{E} = \frac{15\%}{\sqrt{E}} \oplus 0.4\% \qquad \text{for electromagnetic showers}$$

$$\frac{\sigma_E}{E} = \frac{50\%}{\sqrt{E}} \qquad \text{for hadrons}$$

Vertex, central and forward drift chambers provide charged particle detection in the interval $|\eta| < 3.2$. The tracking system does not incorporate a central magnetic field in order to avoid degradating the calorimeter performance by sweeping low-momentum charged particles out of jets and reduce material.

To identify muons, an additional set of tracking chambers are installed surrounding the calorimeters. The momentum of muons is measured in magnetized iron toroids placed between the first two muon chambers. The achieved resolution is $\delta p/p = 0.2 \oplus 0.003\,p$ for the rapidity range $|\eta| < 3.3$.

5 Cross Section Analysis

5.1 Results from the Dilepton Channel

In the dilepton analysis the search for $t\bar{t}$ is done through the process $p\bar{p} \rightarrow t\bar{t} \rightarrow W^+bW^-\bar{b} \rightarrow l^+\nu_l b l^-\bar{\nu}_l\bar{b}$. The topology of these events consists of two oppositely charged high p_T leptons (e or μ), large $\not\!\!E_T$ (signature of the ν's) and two reconstructed jets, not necessary tagged as b's. Backgrounds to this signature originate from Drell-Yan processes ($\gamma, Z^0 \rightarrow e^+e^-, \mu^+\mu^-$), W pair production ($W^+W^- \rightarrow l^+l^- + X$), $Z^0 \rightarrow \tau^+\tau^-$, QCD $b\bar{b}$ production and lepton misidentification.

The CDF sample selection starts by requiring two leptons, one of them being at least an isolated primary or tight lepton. These are electrons in the central calorimeter region ($|\eta| < 1.1$) with $E_T > 20$ GeV and muons in the central ($|\eta| < 0.6$) and extension chambers ($0.6 < |\eta| < 1.1$) with a $p_T > 20$ GeV. In the search for the second lepton a looser set of identification cuts are used.

The event is then subjected to kinematical and topological cuts to reduce further background. A dilepton invariant mass cut around the Z^0 peak ($75 < M_{ll} < 105$ GeV/c^2) reduces backgrounds from Z^0 decays. Figure 4 shows the dielectron invariant mass distribution prior to the Z^0 mass cut. Further dielectron and dimuon backgrounds come mainly from Drell-Yan processes while for the $e\mu$ channel most of the expected background comes from $Z^0 \rightarrow \tau^+\tau^-$, $b\bar{b}$ and lepton misidentification. A cut on the absolute value of $\not\!\!E_T$, $\not\!\!E_T > 25$ GeV, is required as a signature for the undetected neutrinos. For those events with $\not\!\!E_T \leq 50$ GeV the angle between the direction of the $\not\!\!E_T$ and the nearest lepton or jet, $\Delta\phi(\not\!\!E_T, l \, or \, j)$, is required to be less than 20°. This reduces backgrounds from continuum Drell-Yan when jets are nearest to the $\not\!\!E_T$ and from $Z^0 \longrightarrow \tau^+\tau^-$ when leptons are nearest to the $\not\!\!E_T$ direction. Figure 5 shows the acceptance region in the plane $\Delta\phi(\not\!\!E_T, l \, or \, j)$ vs $\not\!\!E_T$.

The absolute dilepton acceptance is defined as the fraction of all $t\bar{t}$ events that pass the dilepton selection criteria. It can be written for the CDF analysis as:

$$\varepsilon_{dil} = \varepsilon_{geom \cdot p_T} \cdot \varepsilon_{ID} \cdot \varepsilon_{isol} \cdot \varepsilon_{topology} \cdot \varepsilon_{two\,jets} \cdot \varepsilon_{trigger}$$

Monte Carlo simulation is used to determine the geometric and kinematic acceptance, $\varepsilon_{geom \cdot p_T}$, the lepton identification and isolation efficiency, ε_{ID} and ε_{isol} and the topological and two jets cut efficiency, $\varepsilon_{topology}$ and $\varepsilon_{two\,jets}$. The trigger efficiency, $\varepsilon_{trigger}$, is obtained from data collected by independent triggers. Its final value is calculated to be:

$$\varepsilon_{dil} = (0.77 \pm 0.08)\%$$

for a top mass of 175 GeV/c^2. About 58% of the total acceptance comes from the $e\mu$ channel, 27% from the $\mu\mu$ and 15% from the ee channel.

A total number of 9 events survived the cuts (7 $e\mu$, 1 $\mu\mu$ and 1 ee). The expected number of background events is calculated to be 2.0 ± 0.4. Background contributions from Drell-Yan lepton

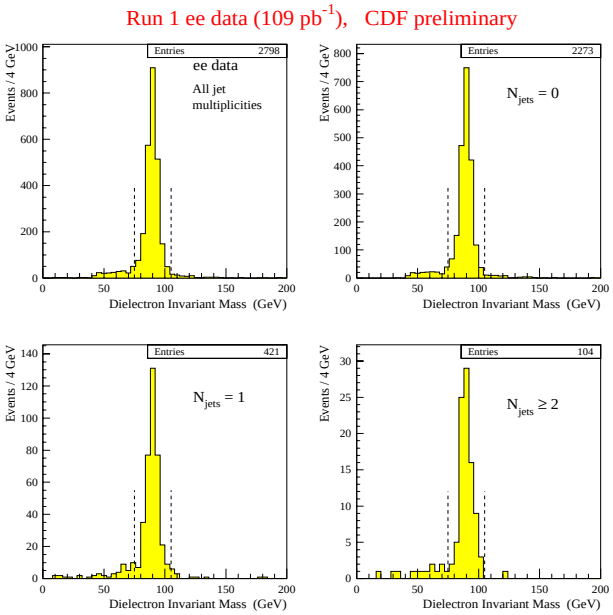

Figure 4: *Dielectron invariant mass distribution prior to the Z^0 mass cut. The different plots are for all jet multiplicities, 0, 1 and ≥ 2 jets. It is clearly evident that the dominant background prior to all cuts are Z^0's.*

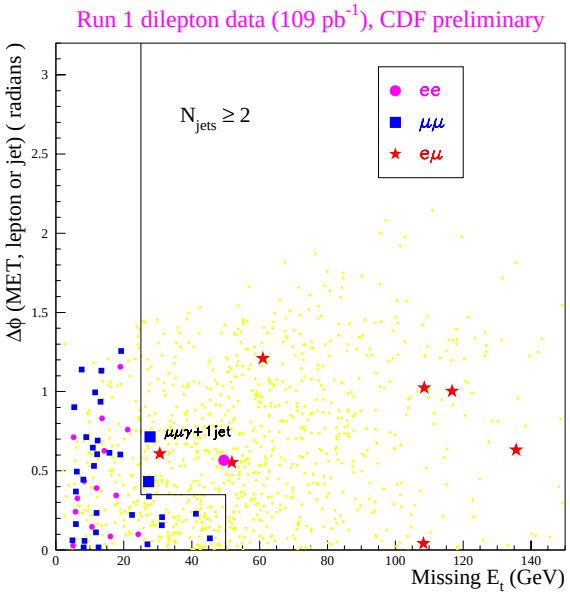

Figure 5: *Topological boundary in the $\Delta\phi(\not\!\!E_T, l \text{ or } j)$ vs $\not\!\!E_T$ plane for the different dilepton channels. Shown also are the distribution of the 9 CDF dilepton candidates. The underlaying points are Monte Carlo top dilepton events.*

pairs, $Z^0 \to \tau^+\tau^-$ and lepton fakes are calculated from data while WW and $b\bar{b}$ production are estimated from Monte Carlo [1, 2]. Tables 2 and 3 show the number of events passing the various consecutive selection requirements on data and the number of background events expected in 110 pb^{-1} respectively. Jets in dilepton events are examined for indications that they originated from b quarks. In the 9 dilepton events 6 jets in 4 events are tagged as b jets. This provides evidence of associated production of W's with b jets, as expected from the decay of the top quark.

The CDF top production cross section from the dilepton yields is measured to be:

$$\sigma_{t\bar{t}}(DIL) = 8.3^{+4.3}_{-3.3}\ pb$$

for a top mass of $M_{top} = 175$ GeV.

The DØ sample selection is similar to CDF although a cut in the H_T variable, $H_T > 120$ GeV, is also applied. H_T is defined as the scalar sum of the transverse energies E_T of the jets ($\mu\mu$ channel) or the scalar sum of the E_T's of the leading electron and the jets ($e\mu$ and ee channels). H_T is found to be a powerful discriminator between background and high mass top quark production.

In order to remove background from Z^0 + jets, additional special cuts are applied by DØ. $Z^0 \to e^+e^-$ background in ee + jet events are removed by asking for $|m_{ee} - m_{Z^0}| > 12$ GeV. DØ momentum resolution is limited by multiple scattering to about 20%. This makes the

	Dilepton Channel		
Dilepton Cut	ee	$\mu\mu$	$e\mu$
Lepton ID	2857	3452	67
Same-Sign	2841	3444	55
Isolation	2798	3357	49
Z^0 Mass	307	369	49
$\not\!\!E_T$	6	6	16
2 jets (10 GeV)	1	1	7
Total CDF Events	9		

Table 2: *Number of CDF data events in the dilepton analysis surviving consecutive requirements.*

$e\mu$	$Z^0 \to \tau^+\tau^-$	0.38 ± 0.11
	WW	0.20 ± 0.09
	Fakes	0.16 ± 0.16
	$b\bar{b}$	0.02 ± 0.02
	Total	0.76 ± 0.21
	CDF Data	7

$ee, \mu\mu$	Drell-Yan	0.61 ± 0.30
	$Z^0 \to \tau^+\tau^-$	0.21 ± 0.08
	Fakes	0.21 ± 0.17
	$b\bar{b}$	0.03 ± 0.02
	Total	1.22 ± 0.36
	CDF Data	2

Table 3: *Number of background events expected in 110 pb^{-1} for the different dilepton channels and number of events in the CDF data sample.*

invariant mass cut to remove $Z^0 \to \mu^+\mu^-$ very inefficient. To remove this background the event as a whole is required to be inconsistent with the Z^0 + jet hypothesis based on a global kinematic fit.

The total DØ yield for $\sim$ 90 pb^{-1} of collected data is 5 events (3 $e\mu$, 1 ee and 1 $\mu\mu$) with an expected background of 1.6 ± 0.3 (see Table 6). Physics backgrounds were estimated by Monte Carlo simulation or from a combination of Monte Carlo and data. Instrumental background from jets misidentified as electrons was estimated completely from data using a rate misidentification probability [3].

5.2 Results from the Lepton + jets Channel

In the lepton + jets decay mode the analysis starts by selecting $W \to e\nu$ and $\mu\nu$ events. The W selection requires an isolated e (or μ) with the same requirements outlined in Section 5.1. In addition a $\not\!\!E_T \geq 20$ GeV is required and Z^0 bosons are removed by rejecting events with an oppositely charged lepton (ee, $\mu\mu$) invariant mass in the range $70 \leq M_{ll} \leq 110$ GeV .

The primary background to the $t\bar{t}$ signal in the lepton + jets mode is direct W + jets production. At least 3 jets with $E_T > 15$ GeV and $|\eta| < 2$ are further required in order to improve the signal to background ratio. This requirement is very efficient in retaining the signal ($\sim 75\%$) while 95% of the events in the W + multijet background are rejected.

In 110 pb^{-1} of data collected by CDF 324 $W + \geq 3$ jet events are found when ~ 38 $t\bar{t}$ events are expected assuming the theoretical predicted cross section and the acceptance for the lepton + $\not\!\!E_T$ + 3 or more jets selection. CDF improves the signal to background ratio by using b-tagging with two different techniques: secondary vertex tagging with the SVX (SVX tagging) and soft lepton tagging (SLT tagging) where an additional lepton from semileptonic b decay is required.

DØ , on the other hand, subdivide the lepton + jet channel (referred to by DØ as single lepton channel) into a b-tagged and untagged channels according to whether or not a muon is observed consistent with the decay $b \rightarrow \mu X$. The muon tagged channels are denoted e+jet/μ and μ+jet/μ.

5.2.1 Secondary Vertex Tagging with CDF

The primary method for finding top quarks in the lepton + jets channel used in CDF relies in looking for secondary vertices from b quark decays. The vertex-finding algorithm searches for secondary vertices with three or more tracks with loose track requirements and, if that fails, searches for two-tracks vertices with more stringent requirements. Using these tracks, the decay length transverse to the beam, L_{xy}, and its error ($\sigma_{L_{xy}} \sim 130$ μm) are calculated using a three dimensional common vertex constrained fit. Jets that have a secondary vertex displaced in the jet direction with a significance $|L_{xy}|/\sigma_{L_{xy}} \geq 3$ are defined to be "SVX tagged".

The efficiency for tagging at least one b jet in $t\bar{t}$ events with at least 3 jets is measured from Monte Carlo simulation to be $(42 \pm 5)\%$. This value is multiplied by a scale factor of 0.87 ± 0.06 in order to agree with the efficiency obtained directly from a control sample, enriched in b decays, of inclusive data electrons.

The expected sources of background events in the W + multijet SVX tagged event sample are: production of W's in association with heavy quark pairs ($Wb\bar{b}$, $Wc\bar{c}$), mistags due to track mismeasurements (fake tags), Wc, $b\bar{b}$ production, WW or WZ production and $Z^0 \rightarrow \tau^+\tau^-$. The background is computed according to the "Method 2" described in [1, 2]. Fake tags backgrounds are obtained directly from data by calculating a tagging rate probability ($-L_{xy}$ parametrization) in a sample of inclusive jet events and applying it to the W + multijet sample before tagging. Background estimation of processes leading to true tags (b or c) are computed separately from Monte Carlo.

Table 4 summarizes the CDF results of the SVX background calculation together with the number of SVX tagged events in ~ 110 pb^{-1} of analyzed data. 42 SVX tags are observed in 34 $W \geq 3$ jet events. The background estimate is measured to be 9.24 ± 1.76 events. Using a

Background Source	W + 1 jet	W+ 2 jets	W + 3 jets	$W + \geq 4$ jets
Mistags (Fakes)	18.7 ± 2.7	6.7 ± 2.6	1.67 ± 0.69	0.67 ± 0.26
$Wb\bar{b}/c\bar{c}$	18.9 ± 7.2	9.6 ± 2.5	2.19 ± 0.62	0.86 ± 0.26
Wc	18.1 ± 5.9	1.4 ± 0.5	0.31 ± 0.13	0.13 ± 0.05
Z + Heavy Flavours	2.7 ± 1.2	1.5 ± 0.5	0.29 ± 0.10	0.05 ± 0.02
$WW, WZ, Z^0 \to \tau^+\tau^-$	1.3 ± 0.4	1.5 ± 0.5	0.29 ± 0.10	0.05 ± 0.02
non-W	7.7 ± 3.5	3.5 ± 1.6	1.28 ± 0.59	0.89 ± 0.41
Total SVX back. events	67.4 ± 13.4	27.2 ± 4.7	6.44 ± 1.18	2.80 ± 0.58
CDF events (before tags)	10716	1663	254	70
CDF events (after tags)	71	45	18	16

Table 4: *Summary of the CDF background composition of the full Run IA+IB W + multijet SVX tagged event sample and observed number of events before and after applying the SVX algorithm on each multiplicity bin.*

total acceptance of $(3.52 \pm 0.65)\%$ evaluated for a $M_{top} = 175$ GeV, the measured cross section in this channel for $t\bar{t}$ production is:

$$\sigma_{t\bar{t}}(SVX) = 6.8^{+2.3}_{-1.8}\ pb$$

5.2.2 Soft Lepton Tagging with CDF

The second technique for tagging b quarks is called Soft Lepton Tagging (SLT) and it looks for additional low p_T leptons from semileptonic b decays through $b \to l\nu_l X$ ($l = e$ or μ) or $b \to c \to l\nu_l X$ (cascade decays). The algorithm matches CTC tracks with electromagnetic energy clusters or hits in the muon chambers.

The efficiency for selecting additional leptons of $p_T > 2$ GeV in top events is estimated from Monte Carlo to be $(20 \pm 2)\%$. A further check of the efficiency of the algorithm is done by applying it on a sample of data electrons from photon conversions and on a sample of muons from $J/\Psi \to \mu^+\mu^-$ decays.

The major backgrounds in the SLT analysis are hadrons misidentified as leptons, electrons from unidentified photon conversions or muons from decays in flight of pions or kaons. Other backgrounds come from W bosons produced with real heavy flavour pairs ($Wb\bar{b}/c\bar{c}$). All these backgrounds (fakes, $Wb\bar{b}/c\bar{c}$) are estimated directly from a track based fake rate derived from a data sample of inclusive jet data. Remaining backgrounds (Wc, diboson production, $b\bar{b}$, Drell-Yan and $Z^0 \to \tau^+\tau^-$) are much smaller and are calculated from a contribution of data and Monte Carlo using the techniques discussed in [1].

The CDF results of the background calculation together with the observed number of SLT tags

on $\sim$ 110 pb^{-1} of analyzed data are shown in Table 5. 44 tags are found on 40 $W+ \geq 3$ jet events. The estimated background is calculated to be 24.6 ± 3 tags. The total acceptance for this method is calculated to be $(1.73 \pm 0.28)\%$ ad the measured cross section is:

$$\sigma_{t\bar{t}}(SLT) = 8.0^{+4.4}_{-3.6}\ pb$$

Figure 6 shows the 42 and 44 observed tags for the SVX and SLT tagging algorithms respectively as a function of the jet multiplicity bin together with the expectations from the different background processes plus $t\bar{t}$ production. In the first and second bin, little contribution from $t\bar{t}$ events is expected. In fact, predicted backgrounds and observed number of events are in good agreement. In the third and ≥ 4 bins a clear excess of tags is observed. Figure 7 shows the proper time and jet E_T distributions for b-tagged jets in the signal region (≥ 3 jets). It is compared with the expected b distributions for $t\bar{t}$ Monte Carlo. The agreement is good.

Background Source	W + 1 jet	$W+$ 2 jets	W + 3 jets	W + $\geq$ 4 jets
Fakes + $Wb\bar{b}$ + $Wc\bar{c}$	239.5 ± 21.8	68.5 ± 6.1	15.7 ± 1.5	7.1 ± 0.7
Drell-Yan	18.9 ± 7.2	9.6 ± 2.5	2.19 ± 0.62	0.86 ± 0.26
$b\bar{b}$	17.7 ± 9.2	2.28 ± 1.2	0.44 ± 0.22	0.14 ± 0.07
Wc	11.2 ± 3.3	4.8 ± 0.73	0.36 ± 0.14	0.08 ± 0.03
WW, WZ	3.9 ± 1.5	1.4 ± 0.5	0.56 ± 0.24	0.25 ± 0.09
$Z^0 \rightarrow \tau^+\tau^-$	4.15 ± 1.72	1.73 ± 1.2	0.4 ± 0.13	0.11 ± 0.36
Total SLT backgr. tags	272 ± 24	78.2 ± 6.9	16.9 ± 2.1	7.7 ± 0.9
CDF SLT tags	245	82	27	17

Table 5: *Summary of the expected CDF background composition of the full Run IA+IB W + multijet SLT tagged sample and observed number of tags after the SLT algorithm on each multiplicity bin.*

5.2.3 The DØ Kinematic and b-tagging Analysis

The signature for the DØ single lepton channels is defined as one isolated lepton, large $\not\!\!E_T$ and three or more jets (when a muon tag is required) or four or more jets (without tag). In the former case a soft muon tag with a minimum $p_T \geq 4$ GeV is required. In addition, a cut on the H_T variable (defined as the scalar sum of the E_T of the jets), $H_T > 110$ GeV and on the aplanarity, $\mathcal{A} > 0.04$ are required. In the second case, a "topological tag" based on more stringent cuts on the H_T and the aplanarity of the jets are required ($H_T > 200$ GeV, $\mathcal{A} > 0.05$). The aplanarity is proportional to the smallest eigenvalue of the momentum tensor of the jets in the laboratory system and ranges from 0 (for planar events) to 0.5 (spherical events).

A total of 32 selected events are observed when adding the four single jet channels together with an expected background of 18.1 ± 2.3 events (see Table 6). The multijet background is

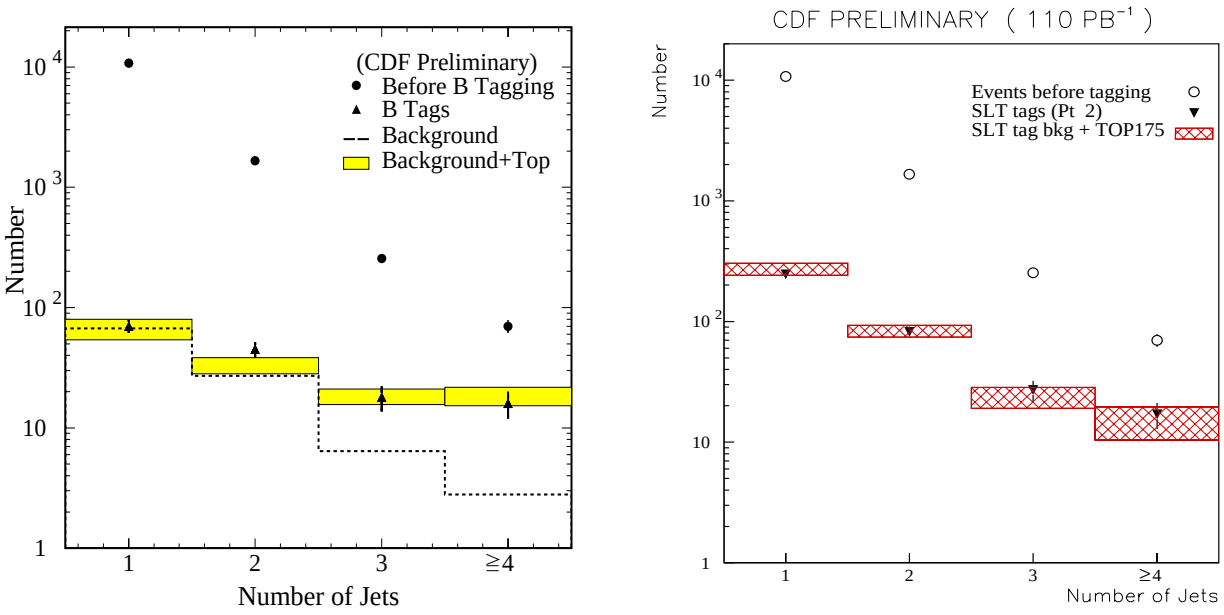

Figure 6: *The W+multijet distribution observed in the CDF data. The circles in both plots correspond to events before tagging and the solid triangles are after SVX tagging (left plot) and after SLT tagging (right plot). Boxes with hatched areas correspond to the background estimates with its uncertainties together with the predicted $t\bar{t}$ contribution.*

estimated directly from data based on a joint probablility of multijet events having large $\not\!\!E_T$ and a jet being misidentified as a lepton [3].

5.3 Results from the All Hadronic Channel

In the all hadronic mode $t\bar{t}$ decays present a topology with 6 jets in the final state with a central jet production of high energy. This data set is dominated by QCD multijet production and the aim of the analysis is then to achieve a reasonable signal-to-background ratio.

The CDF kinematical selection requires a high jet multiplicity, $N_{jets} \geq 5$ where one of which must be b-tagged using the SVX. A total transverse energy $\sum E_T$ is required to be ≥ 300 GeV, deposited mainly in the transverse plane of the detector, $\sum E_T/\sqrt{\hat{s}} \geq 0.75$. In addition, the aplanarity of the event has to satisfy the condition $A \geq -0.0025 \times \sum_3^N E_T + 0.54$ where $\sum_3^N E_T$ does not include the contribution from the 2 leading jets.

Background is estimated directly from data in a similar manner as in the lepton + jets analysis. A tag rate probability is obtained from a sample of inclusive jet events and applied to the data. This sample is supposed to have contributions from real heavy flavour production (direct or through gluon splitting) and tracking mismeasurements.

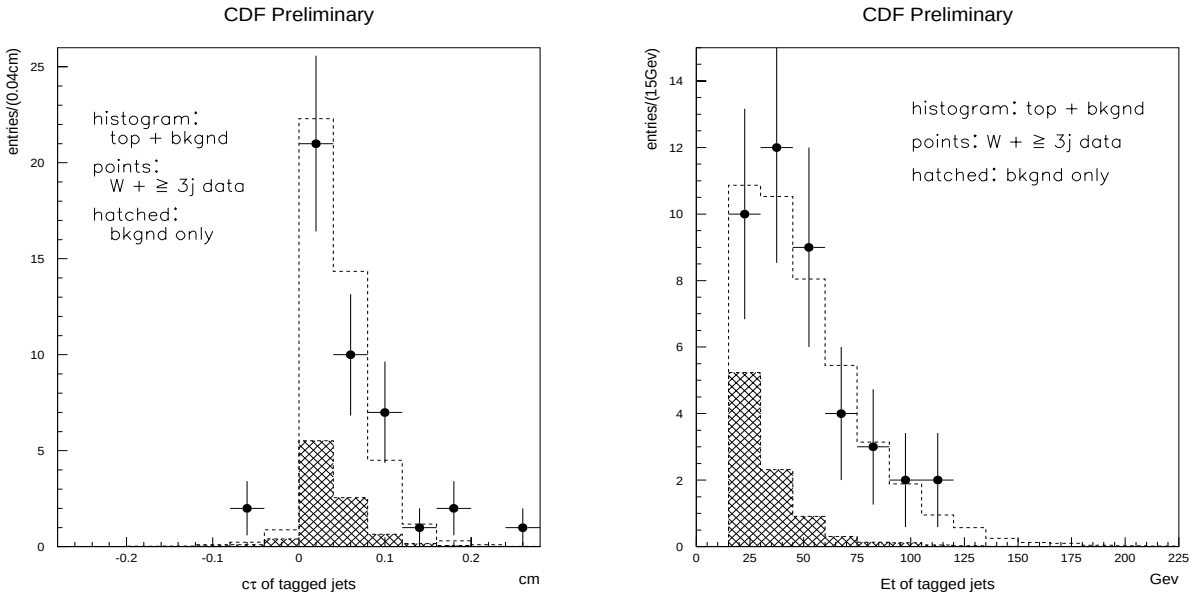

Figure 7: *Proper time distribution (left) and jet E_T spectrum (right) for the b-tagged jets in the signal region ($W+ \geq 3$ jets) in the SVX lepton + jets CDF sample for 110 pb^{-1}. The open histograms shows the expected distributions of b's from a $t\bar{t}$ Monte Carlo simulation with $M_{top} = 175$ GeV. The shaded histograms represents the background in W + jet events.*

A total of 230 tagged jets in 192 events are observed by CDF over a background of 160.5 ± 10.4 tagged jets (147.6 ± 0.7 events) almost entirely from QCD heavy flavour production and mistags. Figure 8 shows the jet multiplicity spectrum for the all hadronic channel. In the 4 jet bin the background and observed tags are in good agreement as one expects because of the small $t\bar{t}$ contribution. A clear excess of tags is observed in the ≥ 5 jet bin.

Using the acceptance of the kinematical requirements for $M_{top} = 175$ GeV which accounts to $(9.9^{+3.0}_{-3.5})\%$ and the b tagging efficiency for this channel, $(47.2 \pm 0.45)\%$, the $t\bar{t}$ production cross section is measured to be:

$$\sigma_{t\bar{t}}(HAD) = 10.7^{+7.6}_{-4.0}\ pb$$

DØ has also reported on the search for $t\bar{t}$ pairs in the all hadronic channel. They start by requiring an initial selection of events at the trigger stage and in the offline analysis. These criteria include $N_{jet} \geq 6$, $E_T > 10$ GeV, $|\eta| < 2$, no isolated leptons ($E_T^e < 20$ GeV, $p_T^\mu < 15$ GeV) and $H_T > 150$ GeV for jets with $E_T > 15$ GeV. Four other additional kinematical parameters are used: the scalar sum of jet E_T excluding the two leading jets (H_T^{3j}), the aplanarity, $\mathcal{A}$, the centrality, $\mathcal{C}$ (given by the ratio of H_T and the sum of all jet energies) and the average number of jets, N_j^{ave}, over a range of E_T thresholds weighted by the E_T threshold. A single or double soft muon tag is also finally required.

15 single μ-tag and 2 double μ-tag data events are observed for an expected background of

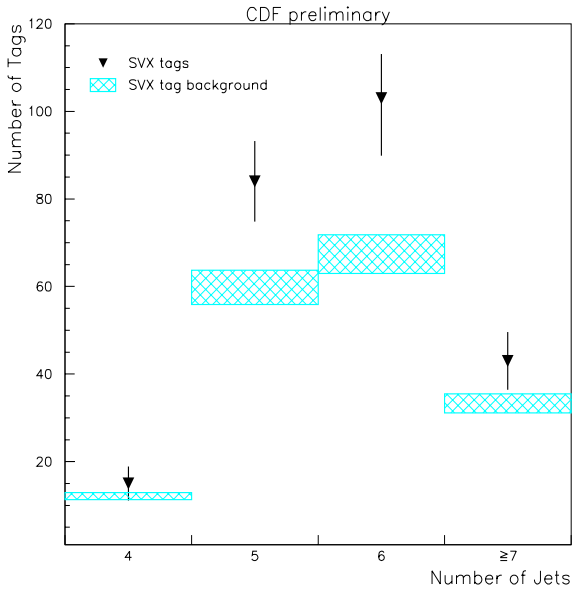

Figure 8: *SVX tagged jet distribution for the all hadronic analysis after kinematical selection as a function of the jet multiplicity compared with the expectation from the background.*

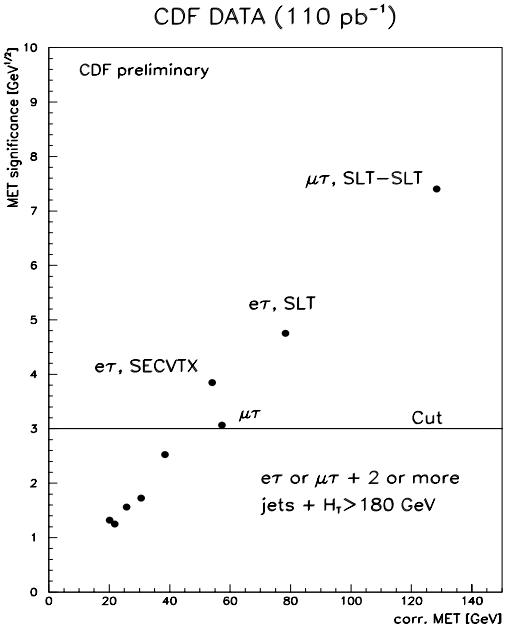

Figure 9: *$\not\!\!E_T$ versus $\sigma_{\not\!\!E_T}$ distribution for a sample of τ-dilepton events in the τ dilepton analysis. The horizontal line represents the cut on $\sigma_{\not\!\!E_T}$.*

11 ± 2 and 1.4 ± 0.4 events respectively. Preliminary values for the cross sections are:

$$\sigma_{t\bar{t}}\,(HAD \text{ single } \mu \text{ tag}) = 4.4 \pm 4.9\ pb$$
$$\sigma_{t\bar{t}}\,(HAD \text{ double } \mu \text{ tag}) = 3.9 \pm 9.8\ pb$$

5.4 τ Dilepton Analysis

CDF has, for the first time, results on evidence of $t\bar{t}$ production in the τ dilepton decay mode. The final state for this topology is one e or μ and a τ identified through its hadronic decays. The primary lepton (e or μ) is selected with the same requirements outlined in the dilepton channel and there is an explicit removal of $Z^0 \rightarrow l^+l^-$ events based on tracking and calorimeter information. The presence of at least two other jets in the event with $E_T \geq 10$ GeV and $|\eta| < 2|$ is also requested. Finally, additional background rejection is obtained with a cut on the H_T variable of the event, $H_T \geq 180$ GeV and on the $\not\!\!E_T$ significance, $\sigma_{\not\!\!E_T} > 3\text{GeV}^{1/2}$, defined as $\sigma_{\not\!\!E_T} = \not\!\!E_T / \sum E_T$.

Although the branching fraction for $e\tau/\mu\tau$ events is the same as for all the dilepton channels together ($\sim 5\%$) the total acceptance for τ dileptons is smaller mainly because of the poor hadronic τ lepton identification. Its final value is measured to be $(0.12 \pm 0.01)\%$ for a top mass of $M_{top} = 175$ GeV.

Channel	$\int \mathcal{L}dt$ (pb^{-1})	Background	Expected Signal	Data
$e\mu$	90.5	0.36 ± 0.09	1.69 ± 0.27	3
ee	105.9	0.66 ± 0.17	0.92 ± 0.11	1
$\mu\mu$	86.7	0.55 ± 0.28	0.53 ± 0.11	1
e+jets	105.9	3.81 ± 1.41	6.46 ± 1.38	10
μ+jets	95.7	5.42 ± 2.05	6.40 ± 1.51	11
e+jets/μ	90.5	1.45 ± 0.42	2.43 ± 0.42	5
μ+jets/μ	95.7	1.13 ± 0.23	2.78 ± 0.92	6
Total:		13.4 ± 3.0	21.2 ± 3.8	37

Table 6: *Preliminary event yields for cross section for each of the counting experiments in the DØ analysis. results include the complete full data sample for Run I. The expected signal has been obtained for a* $M_{top} = 180\ GeV$.

Background sources come from fake hadronic τ decays, $Z^0 \rightarrow l^+l^-$ + jets ($l = e, \mu, \tau$) and dibosons production (WW, WZ^0). The selection yields 4 event candidates with an expected background of 1.96 ± 0.35 events. These 4 events are shown in Figure 9 in the $\not\!\!E_T$ versus $\sigma_{\not\!\!E_T}$ distribution. Given the acceptance outlined above, a preliminary evaluation of the cross section is measured to be:

$$\sigma_{t\bar{t}}(TAU) = 15.6^{+18.6}_{-13.2}\ pb$$

with statistical uncertainties only.

5.5 Combined Results

Using the observed number of candidate events and the acceptances from the dilepton and lepton + jets counting experiments outlined in Section 5, the cross section for $t\bar{t}$ production is measured by CDF to be:

$$\text{CDF:} \quad \sigma_{t\bar{t}}(M_{top} = 175\ GeV) = 7.5^{+1.9}_{-1.6}\ pb$$

The uncertainty is approximately equally divided between the statistical and the systematical contribution. For a detailed description of the combining procedure see [2]. Figure 10 shows the results of the $\sigma_{t\bar{t}}$ for each of the counting experiments individually.

DØ measures the $t\bar{t}$ cross section from their sample of dilepton candidates events, lepton + jets with topological selection events and lepton + jets selected events with b tag requirements. Table 6 shows the event yields for each of the counting experiments corresponding to the full Run I statistics. 37 events are observed in 7 channels with a total expected background of 13.4 ± 3.0 events. The combined preliminary results give:

$$\text{DØ:} \quad \sigma_{t\bar{t}}(M_{top} = 170\,GeV) = 5.2 \pm 1.8\ pb$$

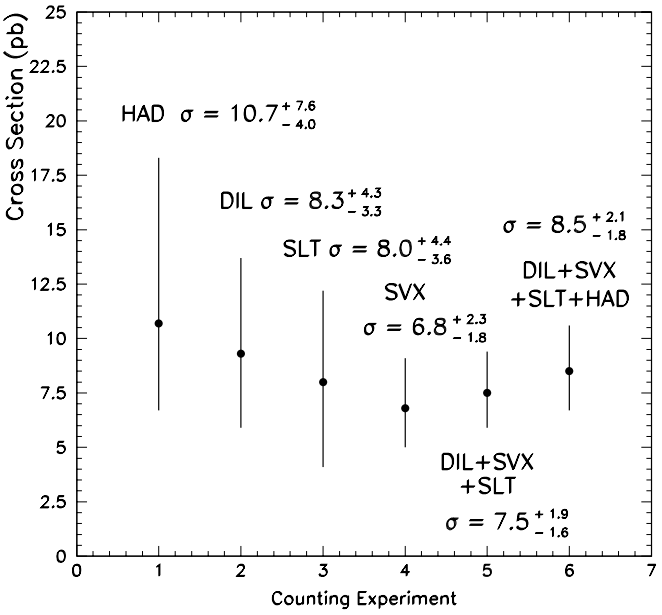

Figure 10: *CDF individual results on $\sigma_{t\bar{t}}$ for each of the counting experiments. Also shown are the combined results for all channels: dilepton (DIL), lepton + jets (SVX, SLT) and all hadronic (HAD).*

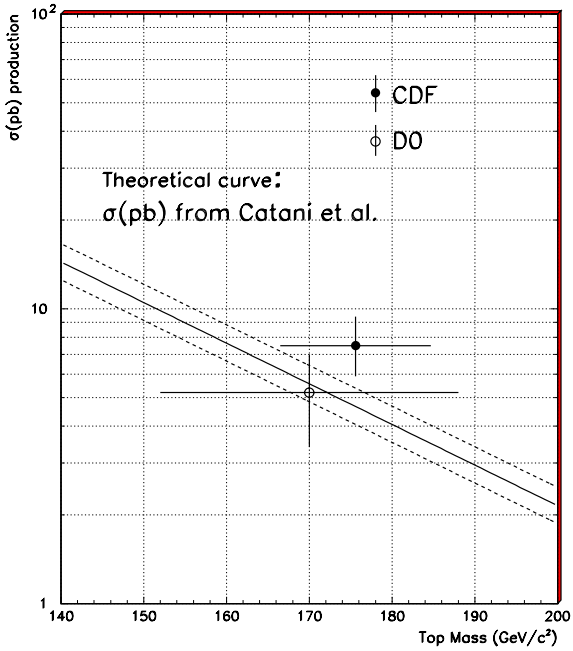

Figure 11: *CDF and DØ individual combined results for the $t\bar{t}$ production cross section as a function of the top mass measurement. Solid line is the theoretical prediction of Catani et al. with errors (dashed lines).*

Figure 11 shows the combined CDF and DØ individual measurements compared to the recent theoretical calculation of Catani *et al.* [7].

6 Mass Measurements

6.1 CDF Mass Analysis

The CDF collaboration measures the top mass with the most accuracy in the lepton + jets channel. Recently, with the analysis of the complete data sample, measurements of the top mass from the dilepton and all hadronic modes have also become possible.

6.1.1 Lepton + jet mass analysis

In the lepton+jets channel the top mass is measured from a sample of lepton + jet events with at least four jets. This will allow a one-to-one matching with the partons from the original $t\bar{t}$ system (two b jets and two hadronic jets from the decay of one of the W's). The fourth jet in the event is required to have $E_T > 8$ GeV and $|\eta| < 2.4$ to enhance the efficiency for detecting

all four jets from the $t\bar{t}$ decay. A total of 153 events is found, 39 of which have at least one jet tagged by the SVX or SLT algorithms.

Each event is then fitted to a $t\bar{t}$ hypothesis with a constrained kinematic fitting procedure where the following system of equations is solved:

$$p\bar{p} \rightarrow t_1 + t_2 + X \qquad \begin{array}{ll} t_1 \rightarrow W_1 + b_1 & W_1 \rightarrow l + \nu \\ t_2 \rightarrow W_2 + b_2 & W_2 \rightarrow j_1 + j_2 \end{array}$$

The tagged jet is assumed to be one of the b's and all other jet assignments are tried. There are also two solutions for the longitudinal components of the ν momenta (p_z^ν). The fit constrains, in addition, the W decay daughters to have an invariant mass equal to the W mass and constrains the t and $\bar{t}$ to have the same mass. From the 5 vertices system mentioned above there are two more constraints than unknowns ("2C" fit). A χ^2 function is then minimized subject to the kinematic constraints for each possible parton-jet assignment. Prior to the fit, all jet energies are corrected in order to account for detector inhomogeneities and energy flows out of the jet clustering cone. The parton assignment leading to the lowest χ^2 solution is selected. The event is rejected if $\chi^2 > 10$. This leaves 34 events with a good kinematic fit.

The background of non-$t\bar{t}$ in the sample is estimated in the same manner as in the cross section analysis. After the mass for each of the fully reconstructed 34 events is determined, this distribution is fit to a superimposition of background plus $t\bar{t}$ using Monte Carlo templates for the shape of the distribution for variable top masses. The background is constrained to the expected number of background events in this sample, which is calculated to be $6.4^{+2.0}_{-1.5}$. A maximum likelihood technique is used to find the best fit value of M_{top}.

Figures 12 and 13 show the reconstructed top mass distribution for events with a lepton and ≥ 4 jets before and after the tagged jet requirement superimposed to the background estimation. Also shown in the inset of Figure 13 is the behavior of the fit likelihood. The fit results on a top mass of:

$$M_{top} = 175.6 \pm 5.7(stat) \pm 7.1(syst) \text{ GeV}$$

The statistical error is obtained from the likelihood fit. The systematic uncertainty comes mainly from the jet energy measurement in reconstructing partons from jets. This accounts for the energy scale uncertainty (cone of 0.4), soft gluon radiation and hard gluon radiation generating extra jets.

The evaluation of the uncertainties relies on the use of Monte Carlo to check its agreement with data in describing the jets. Other sources of systematics arise from using different Monte Carlo generators, different fit configurations, b tagging bias effects on the shapes of the signal and background distributions, background spectrum variations due to different sources of the scale, background free or constrained in the fit and finally, limited Monte Carlo statistics. Figure 16 shows the different sources of systematics with their relative contribution to the final error.

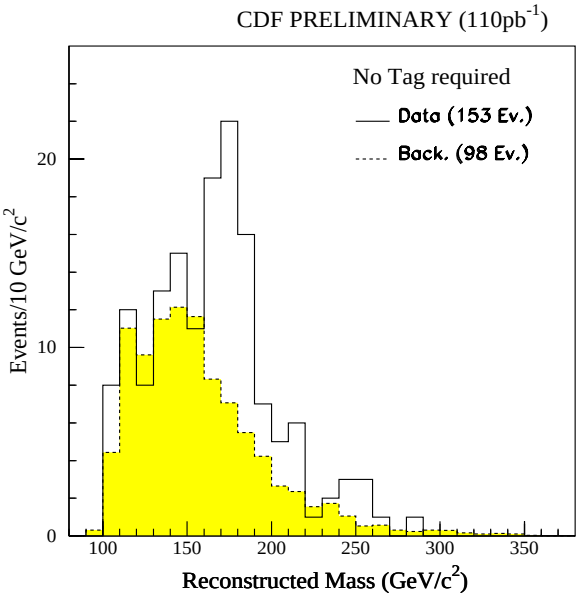

Figure 12: *CDF Run I ($\sim$ 110 pb^{-1} analyzed data) pretagged lepton + jets data sample (solid histogram) compared with the Monte Carlo background (shaded histogram).*

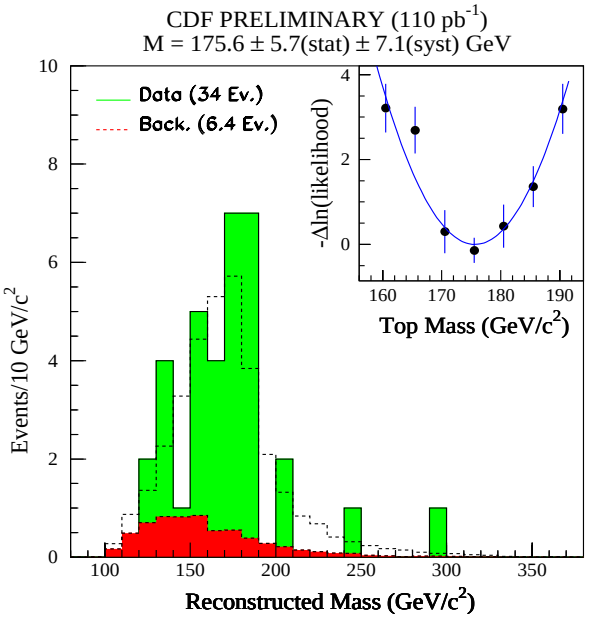

Figure 13: *Fitted lepton + jets b-tagged data sample (black histogram) compared with background (shaded histogram) and background plus top (dashed histogram). The inset shows the normalized Log(likelihood) as a function of the top mas.*

6.1.2 Lepton + jets double tag mass analysis

CDF has also recently measured the top mass with a subsample of the one used in the lepton + jets analysis where two tagged jets are required in the event. Additional cuts on the reconstructed invariant mass of the two untagged jets, $60 \leq M_{jj} \leq 100$ GeV are required for background rejection. This distribution is shown in Figure 14 for the 10 selected events. The mass spectrum shows a clear peak that can be fitted to give a mass of $M_{jj} = 79.8 \pm 4.7$ GeV consistent with the W mass.

A preliminary determination of the top mass using the standard likelihood technique for the 8 events in the W peak results (see Figure 15):

$$M_{top} = 174.8 \pm 7.6(stat) \pm 5.6(syst) \text{ GeV}$$

The sources of systematic uncertainties are shown in Figure 17.

6.1.3 Dilepton mass analysis

In the dilepton channel the presence of a second neutrino in the event makes the simple kinematic fit to the $t\bar{t}$ hypothesis under-constrained. This yields, for each event, a large phase space for possible mass solutions. A method based on the use of kinematical distributions sensitive

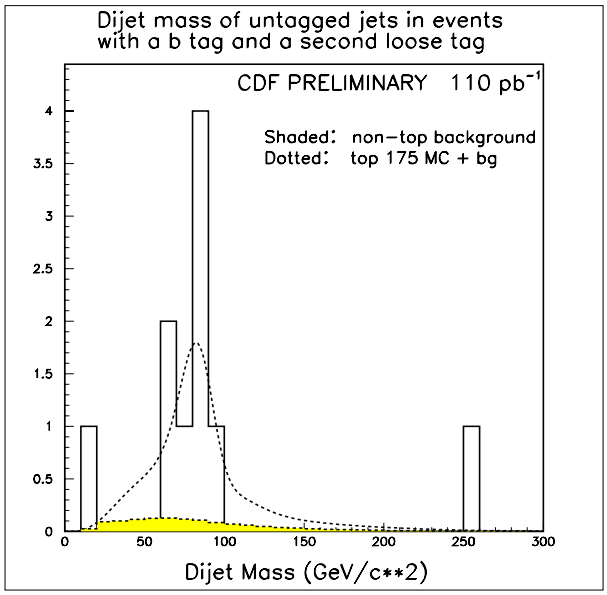

Figure 14: *Dijet invariant mass for untagged jets in double tagged jet events. The peak represents the reconstructed hadronic W. Superimposed are the Monte Carlo expectations for background and top.*

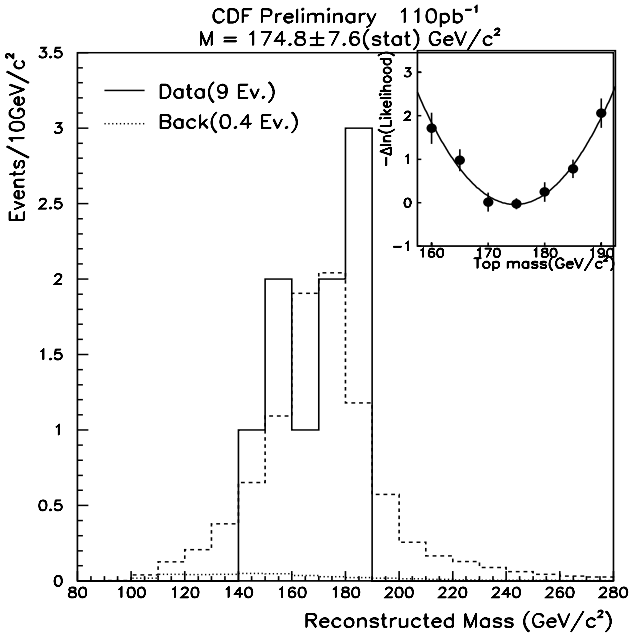

Figure 15: *Reconstructed invariant mass of the fitted double tagged events (solid histogram) with constrained background events. The dashed histogram shows the sum of the $t\bar{t}$ Monte Carlo events and the W+jets background. The dotted histograms represents the background contribution onlt.*

to the top mass is then preferred. The use of the energy of the two leading E_T jets and the total invariant mass of the event are used as kinematical variables. A negative log likelihood fit is performed with different Monte Carlo templates including $t\bar{t}$ and bakground processes.

The data sample used is the same as in the standard lepton analysis with the addition of a cut on the H_T distribution, $H_T > 170$ GeV. Eight data events are remaining with a background of 1.1 ± 0.3 events. Figure 18 shows the distribution of the jet energy for the 8 events and the Monte Carlo expectation. The likelihood fit finds a best mass value of:

$$M_{top} = 159^{+24}_{-22}(stat) \pm 17(syst) \text{ GeV}$$

The systematic uncertainties in the top mass dilepton measurement are tabulated in Figure 20.

6.1.4 All hadronic mass analysis

The mass determination in the all hadronic channel requires at least 6 jets with the remaining cuts identical to those used in the standard analysis. A total of 142 events are left with a background calculated to be 109 ± 7 events. A constrained fit similar to that employed in the

Systematic uncertainties in top mass measurement
CDF PRELIMINARY

Systematics	Value	
	GeV	(%)
Jet E_T Scale	3.1	1.8
Soft Gluon Effects	1.9	1.1
Different Generators	0.9	0.6
Hard Gluon Effects	3.6	2.1
Fit Configuration	2.5	1.4
b-tagging Bias	2.3	1.3
Background Spectrum	1.6	0.9
Likelihood method	2.0	1.1
Monte Carlo statistics	2.3	1.3
Total	7.1	4.0

Figure 16: *Systematic uncertainties for the CDF top mass measurement in the lepton + jets channel.*

Systematic uncertainties in top mass measurement on 2 b-tagged W+≥4jet events

CDF Preliminary 110pb^{-1}

Systematic Uncertainties	values	
	(GeV/c^2)	(%)
Jet E_T Scale	2.9	1.7
Soft Gluon Effects	1.7	1.0
Different Generators	0.9	0.5
Hard Gluon Effects	3.6	2.1
Fit Configuration	0.9	0.5
Tagging Bias	2.0	1.1
Background Spectrum	0.1	<0.1
Likelihood method	0.6	0.3
Monte Carlo statistics	1.0	0.6
Total	5.6	3.2

Figure 17: *Systematic uncertainties for the CDF top mass measurement in the lepton + jets double tagged lepton + jets channel.*

lepton + jets analysis is performed leading to a final result of:

$$M_{top} = 187 \pm 8(stat) \pm 12(syst) \text{ GeV}$$

Figure 19 shows the reconstructed top invariant mass distribution compared to the background estimation. The systematic uncertainties are tabulated in Figure 21.

6.2 DØ Mass Analysis

The DØ collaboration estimates the top quark mass using their sample of single lepton + four jet events subjected to two-constraint + kinematic fits to the hypothesis $t\bar{t} \rightarrow W^+W^-b\bar{b} \rightarrow l\nu q\bar{q}b\bar{b}$ in a manner similar to the CDF analysis described in section 6. Kinematic fits are then performed on all permutations of the jet assignements for the four highest E_T jets. Muon tagged jets are always assigned to a b quark in the fit. A maximum of three permutations with $\chi^2 < 7$ are retained and a single χ^2-probability-weighted average mass ("fitted mass") is calculated per event. 30 of the single-lepton + jet candidate events selected using the standard cuts are succesfully fitted.

An unbinned likelihood fit with top and background contributions is then performed on the fitted mass distribution. The constrained background is found to be 17.4 ± 2.2 for the 30 candidates. The preliminary results of the fit are:

$$M_{top} = 170 \pm 15(stat) \pm 10(syst) \text{ GeV}$$

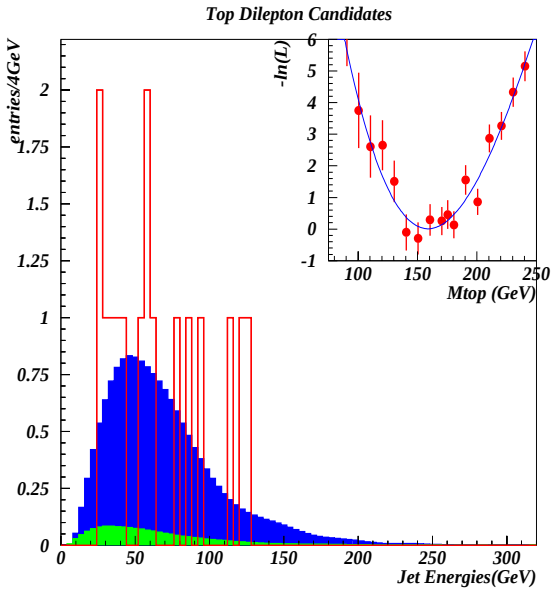

Figure 18: *Jet energy distribution for the selected data events (open histogram) in the dilepton channel compared with the Monte Carlo background expectation (dashed histogram) and a combination of Monte Carlo background and top events.*

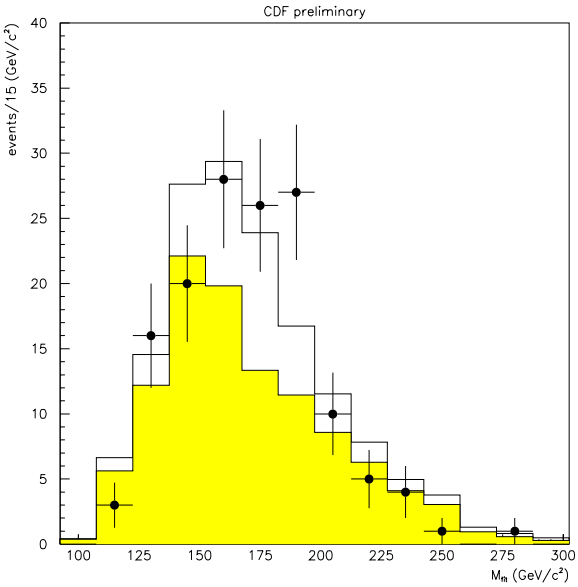

Figure 19: *Reconstructed invariant mass distribution for selected top events in the all hadronic channel (dots). Shaded histogram is the expected background normalized to its estimate. Open histogram is a combination of background plus top Monte Carlo events (M_{top} = 175 GeV).*

The contributions to the systematic uncertainties are the jet energy scale uncertainty (δM_{top} = 7 GeV), event generator dependence and jet definition (6 GeV), different likelihood fitting techniques (3 GeV), background variations (3 GeV) and limited Monte Carlo statistics (1 GeV).

DØ has recently reported on the measurement of the top mass from their sample of 5 dilepton events. Assuming a top mass value, the kinematics of the events may be calculated. A likelihood function is defined as a function of the top mass and a mass estimate for each event is obtained from a maximum likelihood fit. Using the sample of $e\mu$ events (where the background is significantly smaller) the top mass value obtained is:

$$M_{top} = 158 \pm 24(stat) \pm 10(syst) \text{ GeV}$$

CDF: Uncertainties for the Top Mass from Dilepton Events

Source	Error
Statistical Uncertainties:	
Likelihood fit	14.5%
Template statistics	2.0%
Total (statistical)	14.6%
Systematic Uncertainties:	
Jet energy scale	$\leq 10\%$
Background shapes	5%
Structure functions	2%
Different Top MC's	2%
Total (systematics)	11%

Figure 20: *Systematic uncertainties for the CDF top mass measurement in the dilepton channel.*

1996 Behrends' curves used

Systematic	value (%)
Energy scale (Detector effects)	$+2.9, -2.1$
Energy scale (Soft Gluon effects)	± 1.6
Energy scale (Hard Gluon effects)	± 4.3
b-tagging bias	< 0.1
Different background shapes	-1.5
Fit configuration	± 2.1
Likelihood method	$+0.4, -2.4$
Finite template statistics	± 0.3
Fragmentation modeling	$+3.0, -1.0$
TOTAL	$+6.6, -6.3$

Figure 21: *Systematic uncertainties for the CDF top mass measurement in the all hadron channel.*

7 Kinematic Results

In addition to the search techniques based on the counting experiments and outlined in section 5, CDF has also isolated $t\bar{t}$ events based on kinematical properties [8]. From the fit information in the mass subsample analysis, several other properties, apart from the top mass, have been studied in the $t\bar{t}$ system. These represent important checks of the consistency of the $t\bar{t}$ production.

CDF compares data and Monte Carlo for a series of kinematical variables which include the invariant mass and rapidity of the $t\bar{t}$ system ($M_{t\bar{t}}$, $y_{t\bar{t}}$), the p_T and rapidity of the top and the $\Delta\phi$ and Δy between t and $\bar{t}$. This comparison is utilized in the three samples of the lepton + jets mass analysis: the pretagged mass sample, the mass sample and the double tagged mass sample. Figure 22, as an example, shows the invariant mass of the $t\bar{t}$ system and the p_T of the top for the mass sample. The agreement with the Monte Carlo prediction is good.

8 Rare Top Decays and measurement of V_{tb}

CDF has begun to explore the physics of top quark decays. Top branching fractions are of particular interest as they probe the coupling of the top quark to gauge bosons and other quarks. In the Standard Model the CKM matrix element V_{tb} is expected to be close to unity. The branching fraction for top quark decays via $t \rightarrow Wb$ is then $\sim 100\%$. A value smaller that the expected for V_{tb} or $BF(t \rightarrow Wb)$ would indicate the presence of non-Standard Model physics.

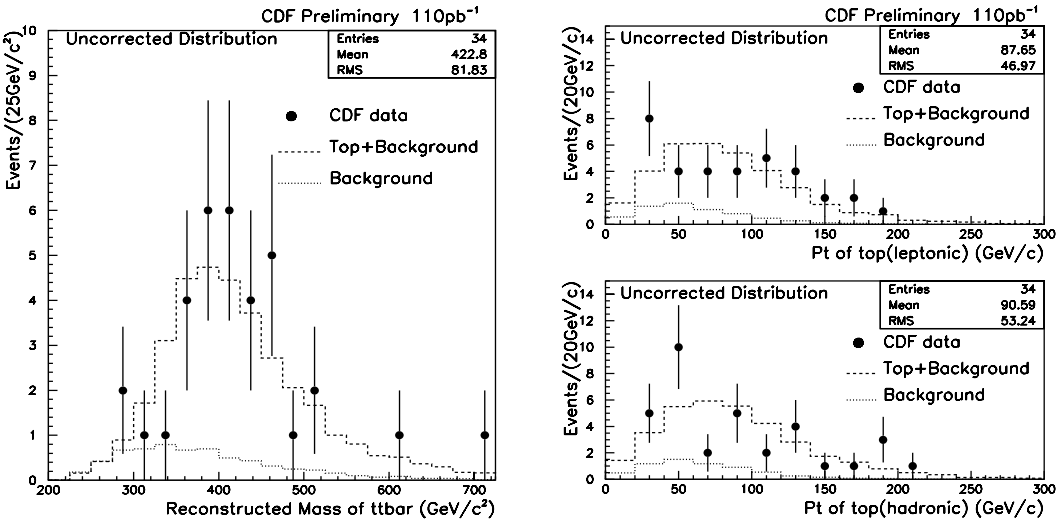

Figure 22: *Invariant mass of the $t\bar{t}$ system (left) and p_T of the top quark associated to the leptonic (upper right) and hadronic (lower right) W. In all cases the tagged mass sample is used.*

CDF measures $BR(t \to Wb)$ using the dilepton sample combined with either the lepton + jets mass sample or a different W + jets sample enhanced in top content by applying kinematic cuts. A maximum likelihood estimator based on the number of observed untagged, single and double tagged events is constructed and the value for the ratio $b = BR(t \to Wb)/BR(t \to Wq)$ which maximizes the likelihood is found. From the observed value for $b = 1.23^{+0.37}_{-0.31}$ a lower limit on $b > 0.61$ at the 95% CL is obtained. Assuming a unitary CKM matrix, $|V_{tb}| = 1.12 \pm 0.16$. Relaxing the unitarity constraint and using the best estimate available for V_{ts} and V_{td} a limit $|V_{tb}| > 0.0502$ (95% CL) is measured.

Supersymmetry predicts many new decays of the top quark, in particular to a charged Higgs boson and a b quark. CDF has also reported on the search for this decay $t \to H^+ b$ where $H \to \tau\bar{\nu}$. Searching in 88 pb^{-1} of Run IB data, 8 events have been observed. This is consistent with the expected Standard Model background (mostly from τ fakes) and has allowed for the exclusion of some regions in the $(M_{H^+}, \tan\beta)$ plane.

CDF has also searched for Flavour Changing Neutral Currents (FCNC) in top decays $t \to Zq$ and $t \to \gamma q$. The branching fractions for these processes are expected to be negligible in the Standard Model ($\sim 10^7 - 10^{12}$). A preliminary limit for the branching fraction $BF(t \to Zq) < 0.44$ at the 90% CL and $BF(t \to \gamma q) < 0.029$ (90% CL) are measured.

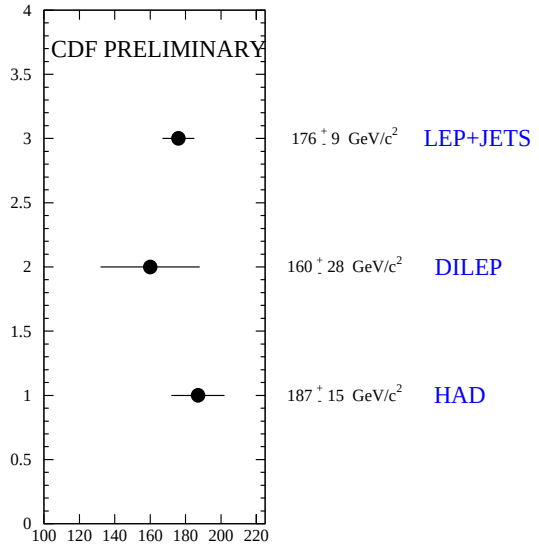

Figure 23: *Summary of the individual preliminary CDF top mass results for each of the different modes analyzed: lepton + jets channel, dilepton channel and all hadronic channel.*

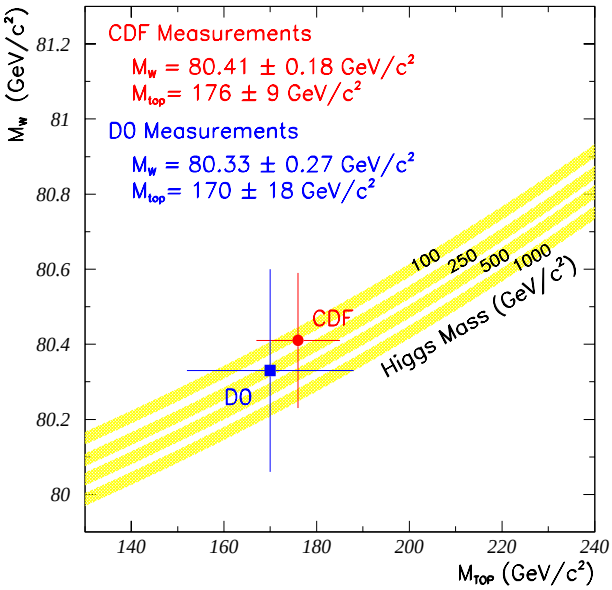

Figure 24: *Top mass as a function of the W mass for the CDF and DØ Run I measurements. Shaded lines are the Standard Model prediction for different Higgs masses.*

9 Conclusions and Future Prospects

Using the complete data set recorded by the CDF and DØ experiments, the latest results on top quark physics at Tevatron have been presented. The large data set available has allowed for detailed studies on top quark production and decay properties. With the analysis of ~ 110 pb^{-1} of data and by utilizing the lepton + jets sample, CDF reports a top mass of:

$$M_{top} = 175.6 \pm 5.7(stat) \pm 7.1(syst) \text{ GeV}$$

Figure 23 shows a summary of other CDF mass measurements, performed in the dilepton and all hadronic sample, for comparison. The combined $t\bar{t}$ production cross section is measured to be:

$$\sigma_{t\bar{t}}\,(M_{top} = 175\ GeV) = 7.5^{+1.9}_{-1.6}\ pb$$

With ~ 100 pb^{-1} of analyzed data DØ reports a top mass measurement of:

$$M_{top} = 170 \pm 15(stat) \pm 10(syst) \text{ GeV}$$

and a combined production cross section of:

$$\sigma_{t\bar{t}}\,(M_{top} = 170\,GeV) = 5.2 \pm 1.8\ pb$$

Figure 24 shows the CDF and DØ top mass results combined with the W mass measurement. This has a direct implication on the mass of the standard Higgs boson.

For the next decade the Tevatron Collider performance will be enhanced by increasing both the instantaneous luminosity (up to $\sim 2 \times 10^{32} cm^{-2} sec^{-1}$) and energy ($\sqrt{s} \sim 2$ TeV). This will be achieved by replacing the Main Ring with the new Main Injector accelerator system.

Both experiments, CDF and DØ , are being upgraded to cope with the smaller bunch spacing of 132 nsec and higher event rates of Tevatron Run II. With an expected integrated luminosity of $\sim 2\ fb^{-1}$, CDF will record on the order of ~ 1500 single SVX tagged $t\bar{t}$ events in the lepton + jets channel if one assumes the improved acceptances of the upgraded detectors. This will allow a measurement of the top quark mass with an uncertainty of ~ 4 GeV. Other physics results expected will be the measurement of the top production cross section with a relative uncertainty of $\sim 9\%$, the observation of single top quark production, the search for anomalously large top rare decays ($BR(t \to c\gamma)$, $BR(t \to cZ^0)$ and $BR(t \to Hb)$) and a large etc.

10 Acknowledgments

I would like to thank the organizers of these conferences for the magnificent atmosphere created and excellent work in the organization. Playa de Gandía was, without any doubt, one of the best possible choices to hold these meetings. I also want to mention and thank all the members of the CDF and DØ collaborations at Fermilab for providing me with the details of their respective analysis. Special thanks to Christianne Ottinger for her careful reading of the manuscript and her support. I also appreciate Jacob Konigsberg for his comments in preparing the document.

References

[1] F. Abe *et al.*, CDF Collaboration, *Evidence for Top Quark Production in $p\bar{p}$ Collisions at $\sqrt{s} = 1.8$ TeV*, **Phys. Rev. Lett. D73** (1994) 225 and **Phys. Rev. D50** (1994) 2966.

[2] F. Abe *et al.*, CDF Collaboration, *Observation of Top Quark Production in $p\bar{p}$ Collisions with the Collider Detector at Fermilab*, **Phys. Rev. Lett. 74** (1995) 2626.

[3] S. Abachi *et al.*, DØ Collaboration, *Observation of the Top Quark*, **Phys. Rev. Lett. 74** (1995) 2632; *Search for High Mass Top Quark Production in $p\bar{p}$ Collisions at $\sqrt{s} = 1.8$ TeV*, **Phys. Rev. Lett. 74** (1995) 2422; *Top Quark Search with the DØ 1992-93 Data Sample*, **Phys. Rev. D52** (1995) 4877.

[4] C.-P. Yuan, **Phys. Rev. D41** (1990) 42; R.K. Ellis, S. Parke, **Phys. Rev. D46** (1992) 3785; D. Carlson, C.-P. Yuan, **Phys. Lett. B306** (1993) 386; S. Cortess, R. Petronzio, **Phys. Lett. B253** (1991) 494; G. Bordes, B. van Eijk, **Nucl. Phys. B435** (1995) 23.

[5] F. Abe *et al.*, CDF Collaboration, *The CDF Detector: an Overview*, **Nucl. Instr. Meth. Phys. Res. A271** (1988) 387.

[6] S. Abachi *et al.*, DØ Collaboration, *The DØ Detector*, **Nucl. Instr. Meth. Phys. Res. A338** (1994) 185.

[7] S. Catani *et al.*, Top Cross Section in Hadron Colliders, CERN TH/96-21, March 21, 1996.

[8] F. Abe *et al.*, CDF Collaboration, *Kinematic Evidence for Top Quark Production in W + multijet events in $p\bar{p}$ Collisions at $\sqrt{s} = 1.8$ TeV*, **Phys. Rev. D51** (1995) 4623.
F. Abe *et al.*, CDF Collaboration, *Identification of Top Quarks Using Kinematic Variables*, **Phys. Rev. D52** (1995) 2605.